

# High-Resolution Adaptive Optics in Vivo Autofluorescence Imaging in Stargardt Disease

Hongxin Song, MD, PhD; Ethan A. Rossi, PhD; Qiang Yang, PhD; Charles E. Granger, MS; Lisa R. Latchney, MS; Mina M. Chung, MD

**IMPORTANCE** Targeting the early pathogenic steps in Stargardt disease type 1 (STGD1) is critical to advance our understanding of this condition and to develop potential therapies. Lipofuscin precursors may accumulate within photoreceptors, leading to photoreceptor damage and preceding retinal pigment epithelial (RPE) cell death. Fluorescence adaptive optics scanning light ophthalmoscopy can provide autofluorescence (AF) images in vivo with microscopic resolution to elucidate the cellular origin of AF abnormalities in STGD1.


**OBJECTIVE** To study the spatial distribution of photoreceptor, RPE, and AF abnormalities in patients with STGD1 at a cellular level.

**DESIGN, SETTING, AND PARTICIPANTS** Cross-sectional study using fluorescence adaptive optics scanning light ophthalmoscopy to compare the cones, rods, and RPE cells between 3 patients with STGD1 and 1 control individual. Imaging sessions were conducted at the University of Rochester. Further image analyses were performed at Beijing Tongren Eye Center and the University of Pittsburgh. Data were collected from August 2015 to February 2016, and analysis began in March 2016.

**MAIN OUTCOMES AND MEASURES** Structural appearance of cones, rods, and AF structures at different retinal locations.

**RESULTS** Two women and 1 man with macular atrophy phenotype of STGD1 and visual acuity loss ranging from 20/30 to 20/150 and 1 woman without STGD1 with 20/20 visual acuity were analyzed. Cone and rod spacing was increased in all 3 patients at all locations where photoreceptors were detectable; most cones had a dark appearance. Autofluorescence was low contrast but contained structures consistent with RPE cells in the periphery. In the transition zone peripheral to the foveal atrophic lesion, the structural pattern of AF was more consistent with photoreceptors than RPE cells. The microscopic AF was disrupted within areas of clinically detectable atrophy.

**CONCLUSIONS AND RELEVANCE** Adaptive optics high-resolution images of cones, rods, and RPE cells at the leading disease front of STGD1 macular atrophy show an AF pattern that appears to colocalize with photoreceptors or may result from a combination of AF signals from both RPE cells and photoreceptors. This in vivo observation is consistent with histologic reports of fluorescence arising from photoreceptors in STGD1. The detection of bisretinoid accumulation in the photoreceptors may represent an early pathologic step in STGD1 and can provide an in vivo imaging tool to act as a biomarker of disease progression.

 **Video and Supplemental content**

*JAMA Ophthalmol.* 2019;137(6):603-609. doi:10.1001/jamaophthalmol.2019.0299  
Published online March 21, 2019.

**Author Affiliations:** Author affiliations are listed at the end of this article.

**Corresponding Author:** Hongxin Song, MD, PhD, No. 2 Chongnei Street, Beijing, China, 100730 (songhongxin2012@163.com); Mina Chung, MD, 601 Elmwood Ave, Box 659, Rochester, NY 14642 (mina\_chung@urmc.rochester.edu).

Stargardt disease type 1 (STGD1), the most common form of early-onset macular dystrophy, is associated with mutations in the ATP-binding cassette transporter (*ABCA4*) gene<sup>1</sup> and is characterized by a spectrum of retinal phenotypes ranging from retinal pigment epithelial (RPE) atrophy in the macula to photoreceptor degeneration across the entire retina.<sup>2</sup> Loss of *ABCA4* function is associated with RPE lipofuscin accumulation and photoreceptor degeneration in mouse models.<sup>3</sup> Histologic investigations have demonstrated increased accumulation of lipofuscin in the RPE and accumulation of lipofuscin precursors within photoreceptors.<sup>4,5</sup> Lipofuscin is a complex aggregate of many different bisretinoids, including A2E.<sup>6</sup> The immediate A2E precursor, A2-PE,<sup>7</sup> is generated in photoreceptor outer segments.<sup>8</sup> The phagocytosis of shed photoreceptor outer segment discs in normally functioning RPE is thought to prevent A2-PE from accumulating within the photoreceptors.<sup>5</sup> However, A2-PE has been shown to accumulate in the photoreceptors of animals that are unable to phagocytose shed outer segments.<sup>9</sup> A2-PE is autofluorescent (AF) at short wavelengths, and it may account for the lipofuscinlike fluorescence of photoreceptors seen histologically in STGD1.<sup>4,7</sup> A pathogenic sequence of lipofuscin accumulation leading to RPE cell damage and subsequent photoreceptor death has been proposed.<sup>10</sup> An alternative hypothesis is that lipofuscin precursors accumulate within photoreceptors, leading to photoreceptor damage simultaneous to or preceding RPE cell death.

Clinical imaging methods, such as confocal scanning laser ophthalmoscopy, have been used to examine the short wavelength fundus autofluorescence (FAF) pattern thought to arise from lipofuscin to assess the status of the RPE in STGD1.<sup>11</sup> In macular atrophy, the most frequently observed phenotype, increased AF accumulation surrounding the margin of RPE atrophy, designated the leading disease front, is considered to represent the earliest disease change in STGD1.<sup>12</sup> Although FAF in confocal scanning laser ophthalmoscopy provides a wide-field view of the regional distribution of lipofuscin AF, morphometric analysis of the RPE cell mosaic is not available using currently available commercial FAF imaging systems because they lack the resolution to identify individual cells. Using AF imaging methods in fluorescence adaptive optics scanning light ophthalmoscopy (FAOSLO), single-cell resolution of RPE cells has been achieved in both healthy<sup>13</sup> and diseased eyes<sup>14-16</sup> in the living human retina; recent advances in our group having greatly increased the efficiency of the approach.<sup>17</sup> Here we use FAOSLO to characterize the cellular level retinal phenotype of rods, cones, and RPE cells in 3 patients with the macular atrophy phenotype of STGD1.

## Methods

This study was designed at beginning of 2015 and approved by the University of Rochester Research Subjects Review Board. Written informed consent was obtained, and participants received financial compensation. Three patients with

## Key Points

**Question** What structures are the sources of the autofluorescence signals in Stargardt disease type 1 (STGD1)?

**Findings** In a cross-sectional study of high-resolution in vivo images of cones, rods, and retinal pigment epithelial cells in 3 individuals with STGD1, the autofluorescence pattern imaged in the transition zone adjacent to clinically detectable retinal pigment epithelial atrophy may arise from photoreceptors or represent a combination of autofluorescence signals from retinal pigment epithelial cells and photoreceptors.

**Meaning** The hyperautofluorescence at the leading disease front in STGD1 may be mediated by the accumulation of lipofuscin precursors in photoreceptors and may represent an early disease step in STGD1.

STGD1 were examined in August 2015, October 2015, and February 2016, respectively; an age-matched participant from a previous study of normal eyes served as a control for comparison. A complete ophthalmic examination, including Snellen visual acuity measurement and dilated fundus examination, was performed. Clinical images were obtained, including color fundus photography (FF450 plus; Carl Zeiss Meditec), conventional FAF in confocal scanning laser ophthalmoscopy, and spectral-domain optical coherence tomography (Spectralis HRA+OCT; Heidelberg Engineering and Cirrus OCT; Carl Zeiss Meditec).

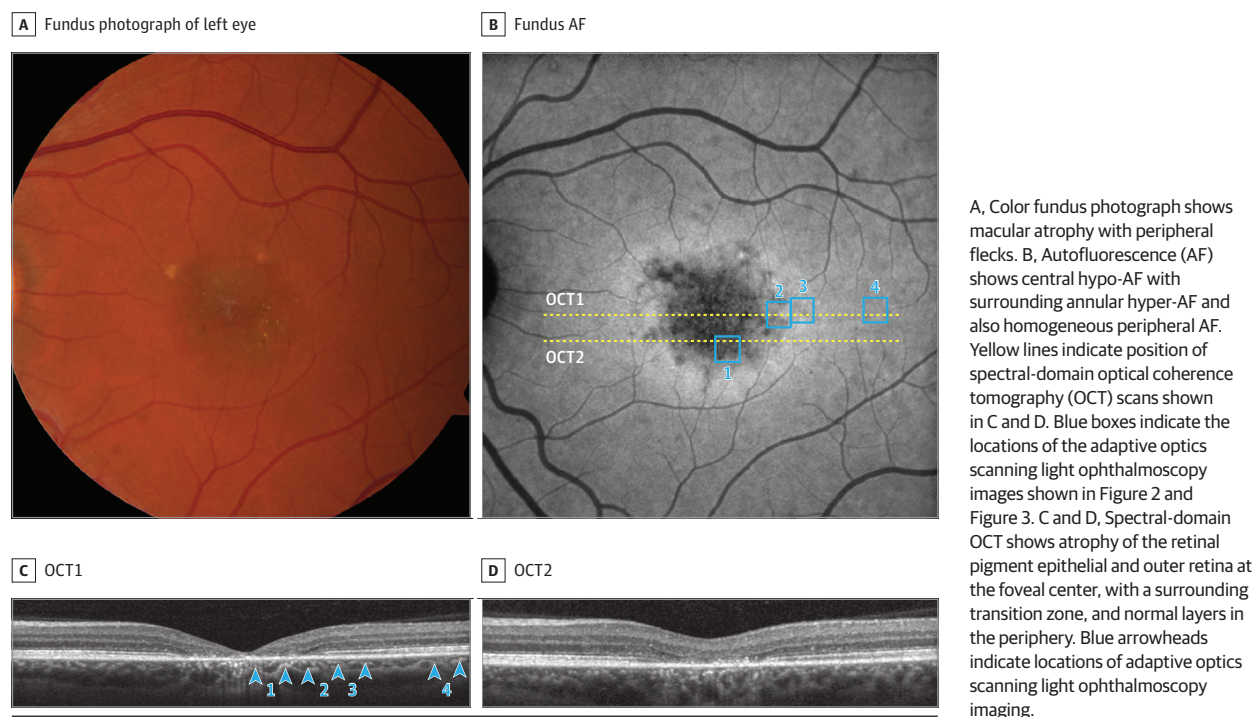
Confocal near-infrared reflectance (max  $\lambda$  = 790; full width at half maximum = 19 nm) and short wavelength AF (excitation = 532 nm; emission = 575 to 725 nm) images were acquired using a technique described previously with recently demonstrated improvements.<sup>16,17</sup> Photoreceptors were marked semiautomatically using previously established methods.<sup>18</sup>

## Results

All 3 patients demonstrated the macular atrophy phenotype of STGD1 with central visual acuity loss. Conventional FAF showed central hypo-AF with surrounding hyper-AF as well as uniform AF peripherally. Spectral-domain optical coherence tomography confirmed atrophy of the RPE and outer retina centrally, with a surrounding annular transition zone, and normal retinal and RPE layers peripherally. Multimodal clinical imaging results of patient 2, a woman in her mid 30s with 20/30 visual acuity, are shown in **Figure 1**. Multimodal clinical imaging results of patient 1, a man in his late 30s with 20/150 visual acuity, and patient 3, a woman in her early 20s with 20/150 visual acuity, are shown in eFigure 1 in the **Supplement**.

Within the macular atrophic lesion, no clearly discernible photoreceptors were identifiable in confocal reflectance images in the patients with STGD1 (**Figure 2** and eFigure 2 in the **Supplement**). In patients 2 and 3, no continuous RPE cell mosaics were identifiable in FAOSLO images near the fovea; only scattered hypo- and hyper-AF was seen at this retinal

Figure 1. Multimodal Imaging of Patient 2



eccentricity (Figure 2D and eFigure 2D in the [Supplement](#)). In patient 1, who had the smallest area of macular atrophy in this series, RPE cell-like structures were identified in reflectance images (eFigure 2A in the [Supplement](#)). Fluorescence adaptive optics scanning light ophthalmoscopy results were abnormal, lacking the characteristic appearance of the RPE mosaic, and its structure was more consistent in appearance with photoreceptor reflectance (eFigure 2B in the [Supplement](#)).

At the transition zone surrounding the macular atrophic lesion, adaptive optics scanning light ophthalmoscopy (AOSLO) showed cones were abnormally dark, enlarged, and sparse (Figure 3 and eFigure 3 in the [Supplement](#)). Cone spacing (Figure 3A) was increased by 50% compared with normal eyes at 1.8 mm (16.2  $\mu$ m vs mean [2 SD], 10.7 [2.9]  $\mu$ m in normal eyes<sup>18</sup>). Rod spacing at the same location was increased by approximately 20% compared with normal eyes (rod spacing was 3.85  $\mu$ m in patients with STGD1 vs 3.2  $\mu$ m in normal eyes), consistent with our previous findings in patients with STGD1.<sup>19</sup> The AF signal appeared abnormal (Figure 3 and eFigure 3 in the [Supplement](#)), lacking the characteristic appearance of the normal RPE mosaic and appearing to colocalize with the photoreceptor reflectance pattern. The [Video](#) shows an overlay comparison of Figure 3C and D. These structures may be composed of photoreceptor and RPE cell debris; some hyper-AF features in this area may represent lipofuscin laden macrophages.

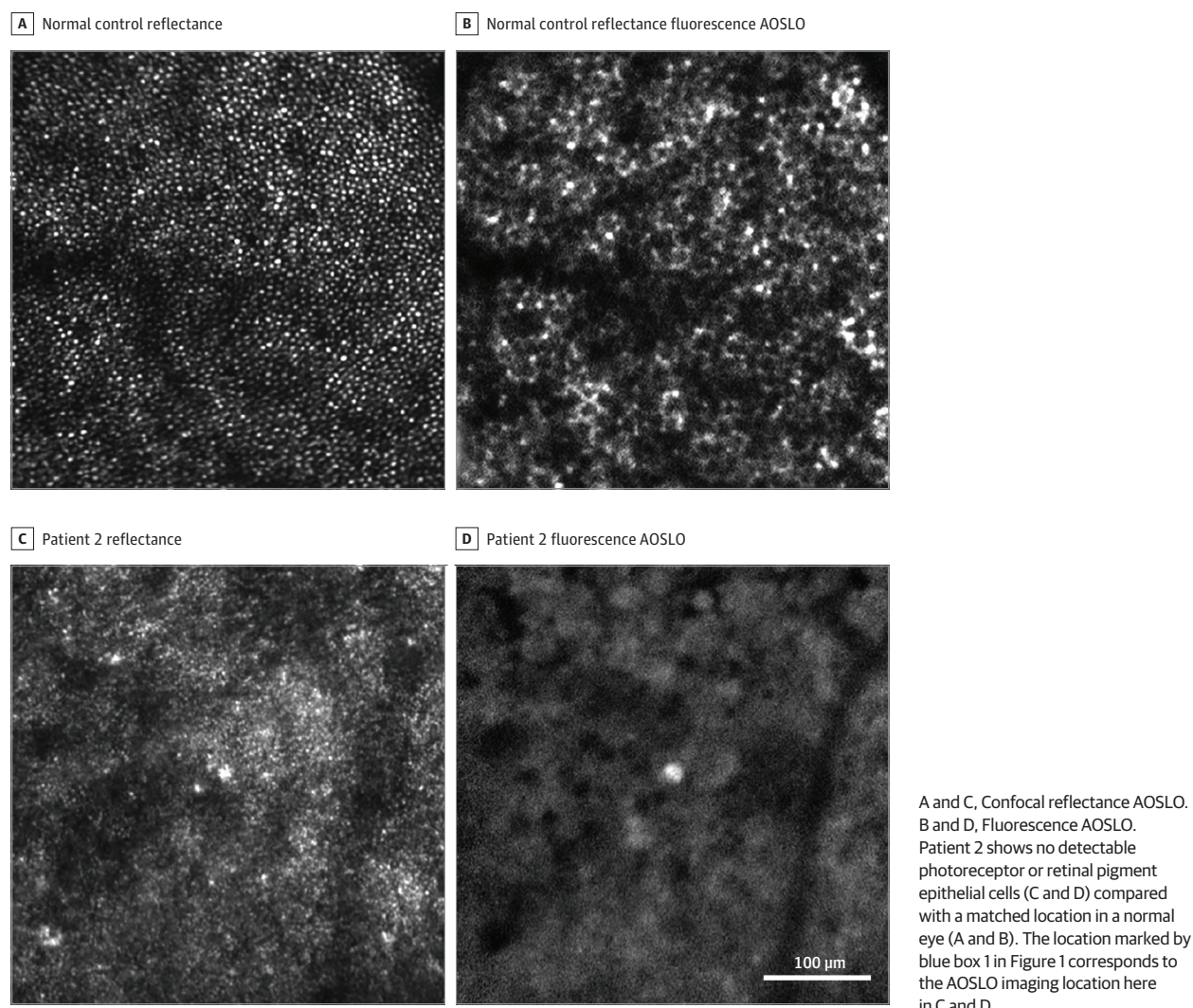
In the retinal periphery, photoreceptor structures were more consistent with the normal expected photoreceptor mosaic appearance and spacing. Fluorescence adaptive

optics scanning light ophthalmoscopy images exhibited an AF pattern consistent with the RPE cell mosaic. However, RPE cell contrast was lower than in normal eyes and the central hypo-AF region of each cell (thought to derive from the absence of lipofuscin in the cell nucleus)<sup>13</sup> appeared qualitatively smaller, with the hyper-AF at the cell margin appearing thicker and less distinct.

## Discussion

This study demonstrates the microscopic distribution and accumulation of the short wavelength AF that underlies the patterns seen in conventional wide-field FAF images of patients with STGD1. Near the fovea, we observed some persisting AF in AOSLO in areas corresponding to markedly reduced FAF in confocal scanning laser ophthalmoscopy. However, the pattern of AF was not characteristic of the normal RPE cell mosaic and these areas were devoid of the normal photoreceptor pattern seen in reflectance AOSLO, suggestive of photoreceptor loss and consistent with spectral-domain optical coherence tomography findings. In the transition zone outside the clinically apparent macular atrophic lesion, cones were sparse, enlarged, and their reflectance diminished; rods were continuous but with increased spacing, consistent with findings in our previous study.<sup>19</sup> Although near the resolution limit of our imaging system and thus difficult to quantify, the rod spacing increase appeared to be driven by an enlarged cell diameter, similar to the enlarged cones that we have shown previously.<sup>19</sup>

Figure 2. Adaptive Optics Scanning Light Ophthalmoscopy (AOSLO) Imaging Near the Fovea (0.5 mm Eccentricity)

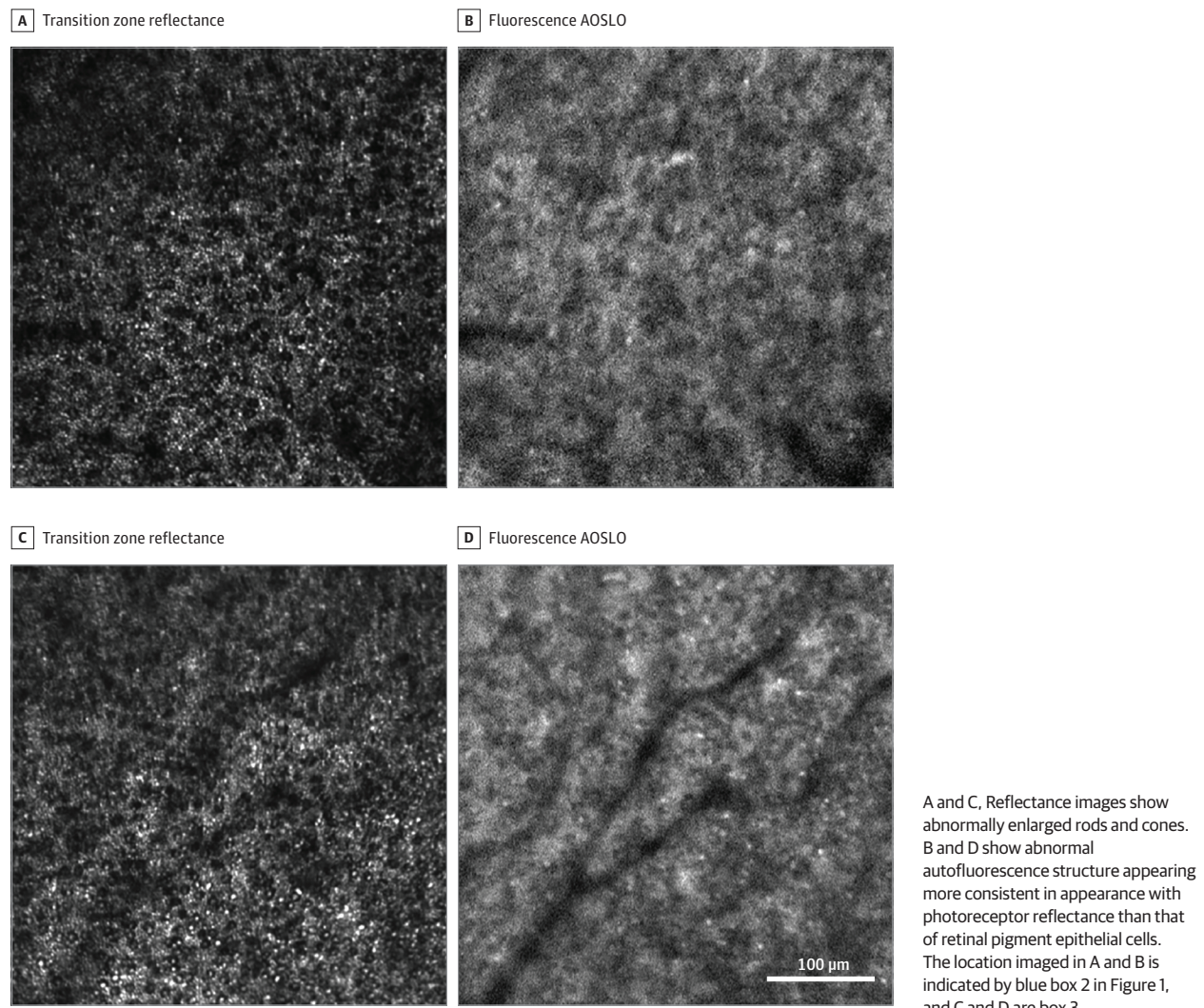


Comparing the photoreceptor layer findings with RPE cell morphometry has yielded additional insight into the temporal sequence of structural abnormalities that accompany cell loss in STGD1. We had previously shown that AOSLO photoreceptor findings were suggestive that photoreceptor loss preceded the clinically detectable RPE loss seen in FAF. Here we can see that despite uniform AF in wide-field FAF images, the underlying RPE morphometry can be quite abnormal, demonstrating that cellular-level AF imaging with AOSLO can reveal RPE morphometric abnormalities that are not detectable in conventional FAF instruments.

The microscopic structural pattern of AF we observed at the transition zone, or leading disease front, just outside the area of hypo-AF seen in wide-field FAF, appeared to correspond to areas where photoreceptors, particularly rods, are present in the confocal reflectance AOSLO images (Figure 3A and B) rather than the characteristic pattern of RPE morphology typically seen. A similar morphology was seen in the area of a hyper-AF ring seen in the wide-field FAF image for

patient 1 and in an area of heterogeneous AF in wide-field FAF in patient 2, demonstrating that the wide-field AF pattern does not uniformly correspond to the abnormalities seen at a microscopic scale. In patient 1 near the fovea, we can see RPE-like structures in the reflectance images similar to a previous report by Roorda et al<sup>20</sup> in patients with cone-rod dystrophy; however, in the AF image at the same retinal location, normal RPE structures are not apparent but rather hyper-AF signal, suggesting the RPE cells are not healthy RPE cells but cells filled with lipofuscinlike AF material. The AF pattern seen in AOSLO suggests that the AF signal may arise either from the photoreceptors or represent a combination of AF signal arising from both RPE cells and photoreceptors. A loss of *ABCA4* function causing the failure of transport of retinoids from the photoreceptors to the RPE would explain our findings that are suggestive of AF signal arising from photoreceptors. This finding is consistent with previous histological evidence of lipofuscinlike AF in photoreceptors<sup>4</sup> and represents evidence of this in vivo.

Figure 3. Adaptive Optics Scanning Light Ophthalmoscopy (AOSLO) Imaging at the Transition Zone of Patient 2



In the retinal periphery, a more typical pattern of RPE cell morphometry was seen with AOSLO, suggesting the RPE cells are present and relatively normal at this eccentricity. However, there were some differences in the appearance of the RPE cells in these areas: there was less contrast from the central hypo-AF region of the cell and cell borders were indistinct. These subtle morphological differences may be associated with an RPE phenotype that is indicative of early RPE dysfunction. The reduced contrast of RPE cells in these areas may also be due to photoreceptor AF but at a reduced level relative to that seen at more central locations where the disease process is more advanced. However, clear photoreceptor disruption was observed at these retinal eccentricities, suggesting that the photoreceptor disruption may occur earlier or be easier to detect than subtle changes in RPE AF (Figure 4 and eFigure 4 in the Supplement).

Our results provide valuable information to identify viable cells, which will play a central role in the selection of patients amenable to gene replacement or other emerging therapies.<sup>21-23</sup> Treatments targeting photoreceptor preserva-

tion or the reduction of the accumulation of bisretinoids such as A2-PE in photoreceptors should be considered for the treatment of STGD1.

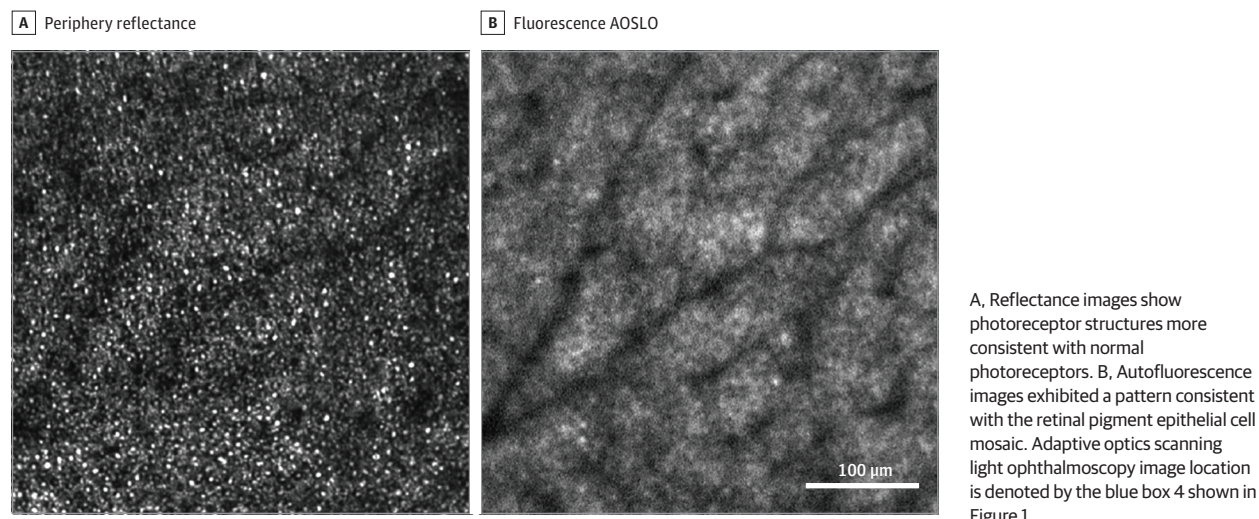
### Limitations

Limitations of this study include the small number of patients with STGD1 imaged and the cross-sectional study design. Imaging of additional patients to confirm these findings, and longitudinal evaluations with FAOSLO may further elucidate the spatiotemporal dynamics and the sequence of cell death in STGD1.

### Conclusions

Adaptive optics scanning light ophthalmoscopy can be used to image photoreceptors and RPE cells in patients with STGD1. High-resolution AF imaging with AOSLO provided insight into the microscopic pattern of AF that underlies the morphologies seen in wide-field FAF. We show here that

Figure 4. Adaptive Optics Scanning Light Ophthalmoscopy (AOSLO) Imaging in the Periphery



uniform hyper-AF and heterogeneous AF in wide-field FAF images can underlie similar patterns of FAF at a microscopic scale that are suggestive of AF arising from both photoreceptors and RPE cells. In the peripheral retina, cone and rod

photoreceptors are disrupted while RPE cells still appear relatively normal suggesting photoreceptor damage mediated by the accumulation of lipofuscin precursors such as A2-PE may precede RPE cell death in STGD1.

#### ARTICLE INFORMATION

**Accepted for Publication:** December 22, 2018.

**Published Online:** March 21, 2019.

doi:10.1001/jamaophthalmol.2019.0299

**Author Affiliations:** Beijing Tongren Eye Center, Beijing Institute Of Ophthalmology, Beijing Tongren Hospital, Capital Medical University, Beijing, China (Song); Beijing Key Laboratory Of Ophthalmology And Visual Sciences, National Engineering Research Center For Ophthalmology, Beijing, China (Song); Center For Visual Science, University of Rochester, Rochester, New York (Song, Yang, Granger, Chung); Department of Ophthalmology, School of Medicine, University of Pittsburgh, Pittsburgh, Pennsylvania (Rossi); Department of Bioengineering, Swanson School of Engineering, University of Pittsburgh, Pittsburgh, Pennsylvania (Rossi); Institute of Optics, University of Rochester, Rochester, New York (Granger); Flaum Eye Institute, University of Rochester, Rochester, New York (Latchney, Chung).

**Author Contributions:** Drs Song and Chung had full access to all of the data in the study and take responsibility for the integrity of the data and the accuracy of the data analysis.

**Concept and design:** Song, Rossi, Chung.

**Acquisition, analysis, or interpretation of data:** All authors.

**Drafting of the manuscript:** Song, Latchney, Chung.

**Critical revision of the manuscript for important intellectual content:** Song, Rossi, Yang,

Granger, Chung.

**Statistical analysis:** Song.

**Obtained funding:** Song, Chung.

**Administrative, technical, or material support:** All authors.

**Supervision:** Song, Chung.

**Conflict of Interest Disclosures:** Dr Rossi reports grants from National Institutes of Health, Canon Inc, Research to Prevent Blindness, and Fight for

Sight during the conduct of the study and reports patents (US 10092181 issued; patent to US patent application No. 14/482195 pending; and patent to US provisional application No. 62/143,341 pending). Dr Yang reports grants from National Institutes of Health National Eye Institute during the conduct of the study and reports patents issued (US-9226656, US-9406133, US-9485383, and US-10092181). Dr Granger reports other support from Canon Inc during the conduct of the study. Dr Chung reports grants from the National Eye Institute and Research to Prevent Blindness during the conduct of the study and grants from Lowy Medical Research Institute, personal fees from Santen Inc, Editas Medicine, and Spark Therapeutics outside the submitted work. No other disclosures were reported.

**Funding/Support:** This work was supported by the National Eye Institute (EY021786, EY021669, EY001319, EY014375, and EY004367), Research to Prevent Blindness, Fight for Sight, Canon Inc, and Capital's Fund for Health Improvement and Research (2018-22-1082).

**Role of the Funder/Sponsor:** The funders provided material and financial support for research but did not specifically dictate the design and conduct of the study, collection, management, analysis, and interpretation of the data; preparation, review, or approval of the manuscript, or decision to submit the manuscript for publication.

#### REFERENCES

1. Allikmets R. A photoreceptor cell-specific ATP-binding transporter gene (ABCR) is mutated in recessive Stargardt macular dystrophy. *Nat Genet*. 1997;17(1):122. doi:10.1038/ng0997-122b
2. Sheffield VC, Stone EM. Genomics and the eye. *N Engl J Med*. 2011;364(20):1932-1942. doi:10.1056/NEJMra1012354

3. Weng J, Mata NL, Azarian SM, Tzekov RT, Birch DG, Travis GH. Insights into the function of Rim protein in photoreceptors and etiology of Stargardt's disease from the phenotype in ABCR knockout mice. *Cell*. 1999;98(1):13-23. doi:10.1016/S0092-8674(00)80602-9

4. Birnbaach CD, Järveläinen M, Possin DE, Milam AH. Histopathology and immunocytochemistry of the neurosensory retina in fundus flavimaculatus. *Ophthalmology*. 1994;101(7):1211-1219. doi:10.1016/S0161-6420(13)31725-4

5. Sparrow JR, Boulton M. RPE lipofuscin and its role in retinal pathobiology. *Exp Eye Res*. 2005;80(5):595-606. doi:10.1016/j.exer.2005.01.007

6. Sparrow JR, Parish CA, Hashimoto M, Nakanishi K. A2E, a lipofuscin fluorophore, in human retinal pigmented epithelial cells in culture. *Invest Ophthalmol Vis Sci*. 1999;40(12):2988-2995.

7. Ben-Shabat S, Itagaki Y, Jockusch S, Sparrow JR, Turro NJ, Nakanishi K. Formation of a nonoxirane from A2E, a lipofuscin fluorophore related to macular degeneration, and evidence of singlet oxygen involvement. *Angew Chem Int Ed Engl*. 2002;41(5):814-817. doi:10.1002/1521-3773(20020301)41:5<814::AID-ANIE814>3.0.CO;2-2

8. Liu J, Itagaki Y, Ben-Shabat S, Nakanishi K, Sparrow JR. The biosynthesis of A2E, a fluorophore of aging retina, involves the formation of the precursor, A2-PE, in the photoreceptor outer segment membrane. *J Biol Chem*. 2000;275(38):29354-29360. doi:10.1074/jbc.M910191199

9. Katz ML, Drea CM, Eldred GE, Hess HH, Robison WG Jr. Influence of early photoreceptor degeneration on lipofuscin in the retinal pigment epithelium. *Exp Eye Res*. 1986;43(4):561-573. doi:10.1016/S0014-4835(86)80023-9

10. Cideciyan AV, Aleman TS, Swider M, et al. Mutations in ABCA4 result in accumulation of lipofuscin before slowing of the retinoid cycle:

a reappraisal of the human disease sequence. *Hum Mol Genet.* 2004;13(5):525-534. doi:10.1093/hmg/ddh048

11. Delori FC, Staurenghi G, Arend O, Dorey CK, Goger DG, Weiter JJ. In vivo measurement of lipofuscin in Stargardt's disease: fundus flavimaculatus. *Invest Ophthalmol Vis Sci.* 1995;36(11):2327-2331.
12. Cideciyan AV, Swider M, Schwartz SB, Stone EM, Jacobson SG. Predicting progression of ABCA4-associated retinal degenerations based on longitudinal measurements of the leading disease front. *Invest Ophthalmol Vis Sci.* 2015;56(10):5946-5955. doi:10.1167/iovs.15-17698
13. Morgan JIW, Dubra A, Wolfe R, Merigan WH, Williams DR. In vivo autofluorescence imaging of the human and macaque retinal pigment epithelial cell mosaic. *Invest Ophthalmol Vis Sci.* 2009;50(3):1350-1359. doi:10.1167/iovs.08-2618
14. Song H, Rossi EA, Stone E, et al. Phenotypic diversity in autosomal-dominant cone-rod dystrophy elucidated by adaptive optics retinal imaging. *Br J Ophthalmol.* 2018;102(1):136-141. doi:10.1136/bjophthalmol-2017-310498
15. Song H, Latchney L, Williams D, Chung M. Fluorescence adaptive optics scanning laser ophthalmoscope for detection of reduced cones and hypoautofluorescent spots in fundus albipunctatus. *JAMA Ophthalmol.* 2014;132(9):1099-1104. doi:10.1001/jamaophthalmol.2014.1079
16. Rossi EA, Rangel-Fonseca P, Parkins K, et al. In vivo imaging of retinal pigment epithelium cells in age related macular degeneration. *Biomed Opt Express.* 2013;4(11):2527-2539. doi:10.1364/BOE.4.002527
17. Granger CE, Yang Q, Song H, et al. Human retinal pigment epithelium: in vivo cell morphometry, multi-spectral autofluorescence, and relationship to cone mosaic. *Invest Ophthalmol Vis Sci.* 2018;59(15):5705-5716. doi:10.1167/iovs.18-24677
18. Song H, Chui TYP, Zhong Z, Elsner AE, Burns SA. Variation of cone photoreceptor packing density with retinal eccentricity and age. *Invest Ophthalmol Vis Sci.* 2011;52(10):7376-7384. doi:10.1167/iovs.11-7199
19. Song H, Rossi EA, Latchney L, et al. Cone and rod loss in Stargardt disease revealed by adaptive optics scanning light ophthalmoscopy. *JAMA Ophthalmol.* 2015;133(10):1198-1203. doi:10.1001/jamaophthalmol.2015.2443
20. Roorda A, Zhang Y, Duncan JL. High-resolution in vivo imaging of the RPE mosaic in eyes with retinal disease. *Invest Ophthalmol Vis Sci.* 2007;48(5):2297-2303. doi:10.1167/iovs.06-1450
21. Charbel Issa P, Barnard AR, Herrmann P, Washington I, MacLaren RE. Rescue of the Stargardt phenotype in ABCA4 knockout mice through inhibition of vitamin A dimerization. *Proc Natl Acad Sci U S A.* 2015;112(27):8415-8420. doi:10.1073/pnas.1506960112
22. Kong J, Kim SR, Binley K, et al. Correction of the disease phenotype in the mouse model of Stargardt disease by lentiviral gene therapy. *Gene Ther.* 2008;15(19):1311-1320. doi:10.1038/gt.2008.78
23. Han Z, Conley SM, Naash MI. Gene therapy for Stargardt disease associated with ABCA4 gene. *Adv Exp Med Biol.* 2014;801:719-724. doi:10.1007/978-1-4614-3209-8\_90